A Tandem Ion Cyclotron Resonance Study of the Reactions of Allyl Ions with Benzene and Substituted Benzene

Raymond Houriet,[1a] Thomas A. Elwood,[1b] and Jean H. Futrell*[1b]

Contribution from the Institut de Chimie Physique EPFL, 1007 Lausanne, Switzerland, and the Department of Chemistry, University of Utah, Salt Lake City, Utah 84112.
Received July 22, 1977

Abstract: Speculation that $C_7H_7^+$ formed in the chemical ionization mass spectra of aromatic compounds coupled with recent detailed studies of the mechanisms of formation of this ion in electron impact mass spectra of alkyl aromatic species have stimulated the investigation of the mechanism of formation of this ion in ion–molecule reactions. A tandem Dempster ion cyclotron resonance mass spectrometer has been used to study the reactions of $C_3H_5^+$ with benzene and seven substituted benzenes. This instrument has also been utilized to investigate long-lived metastable ion decomposition products from the reactions of $C_3H_5^+$ with these compounds. Variation in the chemical preparation of the reactant ion and deuterium and carbon-13 labeling have been used to elucidate details of the mechanism. This combination of techniques supports the hypothesis that both benzyl and tropylium ions are formed in these systems and that they result from the reaction of two different $C_9H_{11}^+$ type intermediates. The competing reactions of proton transfer and hydride ion transfer occur by prompt reaction mechanisms that do not involve isotopic scrambling. Hydride transfer occurs from alkyl side chains. Rate constants for several reacting pairs have been measured; the total rate constant for all reactions is large and comparable to that calculated from simple polarizability theory.

Introduction

The unusual stability of the tropylium ion makes it a highly favored product in gas-phase ion chemistry of alkyl aromatic ions. The cyclic $C_7H_7^+$ structure was initially invoked in the decomposition of alkylbenzenes under electron impact[2a] and has been the subject of numerous investigations.[2b-d] This ion also appears to be a favored product in the reactions of alkyl ions with benzene. An ion cyclotron resonance (ICR) study of chemical ionization (CI) mechanisms by Clow and Futrell[3] showed that $C_7H_7^+$ which was formed in the methane CI spectrum of benzene resulted from the reaction of the $C_3H_5^+$ reagent ion. Clow and Tiernan[4] also studied the formation of $C_7H_7^+$ in the reactions of CH_3^+, $C_3H_3^+$, and $C_3H_5^+$ with benzene in a tandem mass spectrometer experiment. The use of deuterated reactants has shown a pattern for label retention which suggests partial equivalency of the hydrogens in the intermediate reaction complex. However, $C_7H_7^+$ formation was not reported in the earlier high-pressure CI experiments of Munson and Field;[5] rather these authors reported the presence of the addition products $C_8H_{11}^+$, $C_9H_{11}^+$, and $C_9H_{13}^+$ and presumed them to be reaction products of $C_2H_5^+$, $C_3H_5^+$, and $C_3H_7^+$ with benzene.

In order to obtain further information on mechanistic and structural effects favoring the formation of $C_7H_7^+$, we have studied the reaction of $C_3H_5^+$ with benzene in a tandem Dempster–ICR mass spectrometer. $C_3H_5^+$ was formed in the high-pressure mass spectrum of five different gases, providing a wide range of internal energies of reactant ion. By changing the pressure in the ion source, it is possible to collisionally relax the internal energy of the $C_3H_5^+$ ion. Isotopically labeled (^{13}C and D) allyl ions were also used, as well as deuterated neutrals to clarify details of the reaction. In another experiment, the $C_9H_{11}^+$ intermediate complex was formed in the ion source containing a 1/100 mixture of C_6H_6/C_2H_4 at higher pressures and the decomposition of the $C_9H_{11}^+$ was followed in the second stage of the instrument. Finally, substituted benzenes were used as target molecules to investigate the formation of homologues of the tropylium ion.

Experimental Section

The tandem mass spectrometer used in this study has been described in detail elsewhere[6] and will be discussed only briefly here. The first stage of the instrument consists of a 180°, 5.7-cm radius Dempster mass spectrometer, with a high-pressure source working efficiently up to approximately 100 mTorr. The mass analyzed ions are decelerated to approximately thermal energy as they enter the two-section ICR cell where reaction and analysis of the products occur. Relative ion intensities are determined using a conventional oscillator-detector which has been calibrated at different frequencies.

Results and Discussion

A. Product Distributions and Total Rate Constants. Reaction of $C_3H_5^+$ with benzene forms two products, the protonated benzene and the $C_7H_7^+$ ion, according to reactions R-1 and R-2.

$$C_3H_5^+ + C_6H_6 \rightarrow C_6H_7^+ + C_3H_4 \qquad \Delta H_r, \text{ kJ/mol}^7: \ 0 \qquad \text{(R-1)}$$

$$C_3H_5^+ + C_6H_6 \rightarrow C_7H_7^+ + C_2H_4 \qquad \begin{cases} -67 \text{ (benzyl)} \\ -96 \text{ (tropylium)} \end{cases} \qquad \text{(R-2)}$$

The reaction energetics refer to ground-state reactant and product ions. In the present work the reactions of excited allyl ions generated in highly exothermic reactions was investigated. Five different gases were used as sources of allyl ions; Table I gives the associated reaction enthalpies for the formation of $C_3H_5^+$ from each of the gases. Varying the source pressure decreases the internal energy distribution of the allyl ion by collisional relaxation. As this occurs, the ratio of the products of reactions R-1 and R-2 changes in a corresponding manner. The relative intensity of the $C_7H_7^+$ ion is reported in the main portion of Figure 1 as a function of $\bar{n}$, the average number of collisions encountered by allyl ions in the source for the five cases studied (for further discussion of $\bar{n}$, see ref 8). When CH_4, C_2H_6, C_3H_8, and i-C_4H_{10} were used as the source of allyl ions, the product distribution shows a similar dependence on source pressure. That is, the more exothermic channel (reaction R-2) is favored as the number of energy relaxing collisions, $\bar{n}$, increases. Moreover, the C_2H_6 case shows the strongest pressure dependence, in accordance with the fact that the reaction for formation of $C_3H_5^+$ in ethane (from vinyl and acetylene ion precursors) is the most exothermic of the cases studied here (see Table I).

In contrast with the alkane source ion chemistry, the use of C_2H_4 as a source of allyl ions gave quite unexpected results. Here, the highest relative abundance of $C_7H_7^+$ is observed at

0002-7863/78/1500-2320$01.00/0

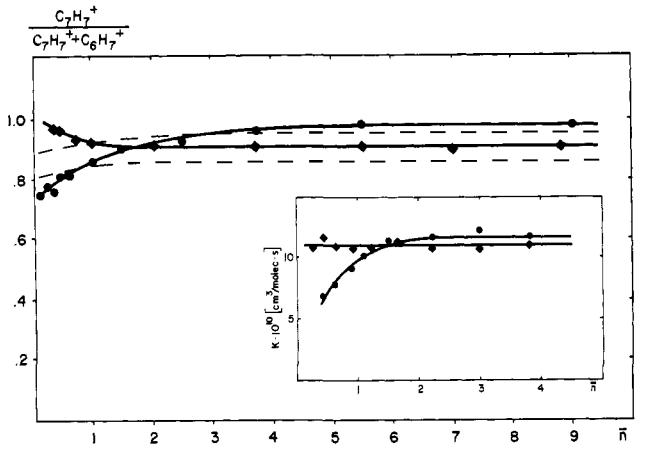

Figure 1. Reaction of $C_3H_5^+ + C_6H_6$: relative intensity of the $C_7H_7^+$ ion and total rate constant k (insert) as a function of $\bar{n}$, the average number of collisions for the reactant ion before extraction from the source. Source of $C_3H_5^+$: ●, C_2H_6; ♦, C_2H_4; -- (upper), CH_4; -- (lower), C_3H_8 (i-C_4H_{10} identical).

Table I. Summary of Reactions for Forming Allyl Ions

Source gas	Ion precursor of the allyl ion	Enthalpy of reaction forming $C_3H_5^+$ ΔH_r, kJ/mol
CH_4	$C_2H_3^+$	−69
C_2H_4	$C_2H_4^+$	−33.5
C_2H_6	$C_2H_2^+$	−163
	$C_2H_3^+$	−176
C_3H_8	Primary ion	
i-C_4H_{10}	Various fragment ions	

the lowest $\bar{n}$, thus showing an inverse behavior to the alkane ion experiments. Except for the protonated parent, other product ions, either fragment or adduct ions, were not formed over the range of pressures studied. Measurements on several

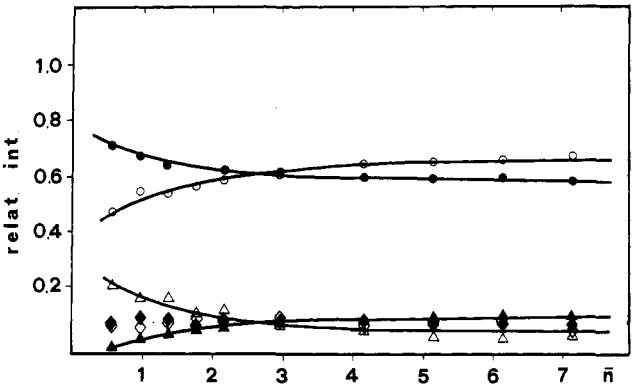

Figure 2. Reaction of $C_3H_5^+ + C_7H_8$; product distribution as a function of $\bar{n}$. Source of $C_3H_5^+$: C_2H_6 (open symbols), C_2H_4 (solid symbols). Product ion: $C_8H_9^+$, ○ ●; $C_7H_9^+$, △ ▲; $C_7H_7^+$, ◇ ♦.

monosubstituted benzenes (C_6H_5X, X = F, CH_3, Cl, OCH_3) and the isomeric xylenes resulted in generally similar ion source pressure dependences to those illustrated in Figure 1 for reactions R-1 and R-2. The relative intensities of the products of the reaction of $C_3H_5^+$ with toluene as a function of source pressure are reported in Figure 2, when C_2H_4 and C_2H_6 are used as sources of allyl ion.

In addition to reactions R-1 and R-2, toluene and the three isomeric xylenes were found to yield hydride transfer products according to the reaction

$$C_3H_5^+ + RC_6H_4CH_3 \rightarrow C_3H_6 + RC_6H_4CH_2^+ \quad \text{(R-3)}$$

where R = H or CH_3. Reaction R-3 is exothermic by about 84 kJ/mol for both toluene and the xylenes. The corresponding reaction is not observed for benzene neutrals because of its high endothermicity (about 188 kJ/mol) in the absence of alkyl side chains.

The total rate constants for reaction of $C_3H_5^+$ with benzene and substituted benzenes are given in Table II (columns 3 and 4), together with the product distributions (columns 6, 11, and

Table II. Reactions of $C_3H_5^+$ [a] with Benzene Derivatives

		Total rate constants [b]		Product branching ratio for neutral eliminated							
				(5)	(6)	(7)	(8)	(9)	(10)	(11)	(12)
(1) Neutral	(2) + ion	(3) k_{tot}	(4) k_{Lang} [c]	d $^{13}CCH_4$	d C_2H_4	d C_2DH_3	d $C_2D_2H_2$	d C_2D_3H	d C_2D_4	e C_3H_4	f C_3H_6
C_6H_6	$+ C_3H_5^+$	11.5	15		0.905					0.095	
	$+ {}^{13}CC_2H_5^+$			0.69	0.31						
	$+ C_3D_5^+$						0.07	0.58	0.35		
C_6D_6	$+ C_3H_5^+$				0.24	0.63	0.13				
C_6H_5F	$+ C_3H_5^+$	15	15		0.91					0.09	
	$+ C_3D_5^+$						0.06	0.58	0.36		
C_6H_5Cl	$+ C_3H_5^+$	15	15.5		0.92					0.08	
	$+ C_3D_5^+$						0.05	0.58	0.37		
$C_6H_5OCH_3$	$+ C_3H_5^+$	15	16.5		0.78					0.22	<0.005
	$+ C_3D_5^+$					<0.005	0.18	0.52	0.30		
$C_6H_5CH_3$	$+ C_3H_5^+$	14.5	16.5		0.72					0.15	0.13
	$+ {}^{13}CC_2H_5^+$			0.65	0.35						
	$+ C_3D_5^+$					0.03	0.15	0.54	0.28		
$C_6D_5CD_3$	$+ C_3H_5^+$				0.22	0.50	0.22	0.06			
o-$C_6H_4(CH_3)_2$	$+ C_3H_5^+$	16	17.5		0.50					0.22	0.28
	$+ C_3D_5^+$				<0.005	0.10	0.24	0.44	0.22		
m-$C_6H_4(CH_3)_2$	$+ C_3H_5^+$	16	17.5		0.47					0.20	0.33
	$+ C_3D_5^+$				<0.005	0.10	0.24	0.44	0.22		
p-$C_6H_4(CH_3)_2$	$+ C_3H_5^+$	15	17.5		0.47					0.20	0.33
	$+ C_3D_5^+$				<0.005	0.10	0.24	0.44	0.22		
Calcd for (5 + 2) stat [g]							0.286	0.571	0.143		

[a] Ethylene source gas. [b] In units of 10^{-10} cm³/molecules. [c] Calculated from $k_{Lang} = 2\pi e(\alpha/\mu)^{1/2}$. [d] Fractions of tropylium (or substituted tropylium) ion formation. [e] Proton transfer. [f] Hydride transfer. [g] Calculated for model assumed in reaction R-4. See discussion in text.

12) determined at a source pressure corresponding to an average of six collisions of the $C_3H_5^+$ ions. Under these conditions, all reactions proceed at a fast rate, very close to that calculated using the simple induced dipole model (k_{Lang}). Thus the measured rate constants are independent of substitution on the benzene ring, in contrast to what is generally observed in the electrophilic substitution reactions studied in the condensed phase.[9]

The total rate constants for reaction of $C_3H_5^+$ with benzene were determined as a function of source pressure for C_2H_4 and C_2H_6 as sources of $C_3H_5^+$; the results are summarized in the insert of Figure 1. When C_2H_4 is the source of allyl ions, the measured rate constant does not change significantly over the range of pressures studied. On the other hand, when C_2H_6 is used to produce allyl ions, the rate constant shows an increase of about 50% with pressure—that is, with decreasing internal energy of $C_3H_5^+$ ions. This increase in reactivity involves only the reaction of $C_3H_5^+$ to form $C_7H_7^+$ (reaction R-2). As will be seen later, reactions R-1 and R-2 apparently proceed via two independent mechanisms.

B. Isotopically Labeled Reactants. The product distributions of the reactions using isotopically labeled reactant ions and/or neutrals are reported in Table II, columns 5-10. In the following discussion, it is assumed that $C_7H_7^+$ formation takes place via a $C_9H_{11}^+$ intermediate complex which loses an ethylene moiety. The experiments using the perdeuterated allyl ion ($C_3D_5^+$) show that in the case of benzene, fluoro-, and chlorobenzene as neutrals, the label retention in the $C_7H_7^+$ ion is identical within experimental error. It is seen that two aromatic hydrogen atoms only are lost in the ethylene neutral. This suggests reaction scheme R-4 for the formation of the $C_7H_7^+$ product.

$$C_3H_5^+ + C_6H_6 \rightarrow \left[\text{I}\right] \rightleftharpoons \left[\text{II}\right] \rightarrow C_7H_7^+ + C_2H_4 \qquad \text{(R-4)}$$

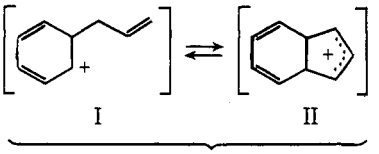

If we assume that the two aromatic hydrogen atoms and the five hydrogens of the reactant ion interconvert rapidly, then decomposition of the $C_9H_{11}^+$ intermediate of structure II would yield the label retention as given under "(5 + 2) statistical" in Table II. It is seen that the contribution of the formal loss of C_2D_4 is always larger than expected from decomposition of structure II only. This is not readily understandable in terms of an isotope effect; therefore, we must assume that a part of $C_7H_7^+$ may be formed directly from structure I of the $C_9H_{11}^+$ intermediate. We can estimate that the latter process is responsible for about 20% of the $C_7H_7^+$ formation.

The question arises as to whether it is possible to assign different structures to the $C_7H_7^+$ ions formed from intermediates I and II. Some evidence relating to this issue is provided by the results for toluene and the xylenes (with $C_3D_5^+$). Here the measured distributions suggest the participation of the methyl hydrogens in the process of mixing of the hydrogen atoms in the reaction intermediate. This is probably related to the formation of products having a substituted benzyl ion structure. From the results obtained with xylene, we can approximate the latter fraction as about 20–30% of the total $C_9X_{11}^+$ production (X = H, D). It is plausible to identify this fraction with the 20% of $C_7H_7^+$ ions formed from reaction with benzene via intermediate structure I. Further, it is reasonable to assume that the $C_7H_7^+$ product should have the benzyl ion structure initially.

The nature of the $C_7H_7^+$ ion has long been an intriguing subject in mass spectroscopy. From the perspective of its decomposition products in a mass spectrometer, isotopic labeling studies show $C_7H_7^+$ to behave as if all its carbon atoms and hydrogen atoms are equivalent during the fragmentation process. The tropylium ion structure is therefore invoked to rationalize these observations.[10] On the other hand, collisional activation[2b] experiments lead to an estimate that the ratio of the structures constituting the $C_7H_7^+$ ion benzyl/tropylium is about 0.3 for ions which initially have insufficient energy for further decomposition. It is of interest that this ratio is in excellent agreement with the rough evaluation of this ratio in the present experiment (0.25–0.33).

This ratio may be qualitatively accounted for by postulating pseudoequilibrium between the hypothetical structures I and II. Since the tropylium ion is more stable than the benzyl ion, its formation is favored by the lowered activation energy for the dissociation process. This argument has also been considered by Dunbar when $C_7H_8^+$ is photodissociated to yield $C_7H_7^+$.[11] It seems to be a satisfactory rationalization for the elimination of ethylene from the intermediate complex of the ion–molecule reactions under investigation.

The extent of label retention observed when $C_3H_5^+$ reacts with perdeuterated benzene and toluene is also summarized in Table II. Except for a reasonable isotope effect, the data parallel the results shown for $C_3D_5^+$ with benzene and toluene; no significant changes were observed when the source pressure was varied or when C_2H_6 was used as an alternate source of $C_3H_5^+$.

The label retention in the $C_7H_7^+$ ion obtained with ^{13}C-labeled allyl ion is reported in columns 5 and 6. The $^{13}C^{12}C_2H_5^+$ ion was formed in the low-pressure ionization of 1-bromo[2-^{13}C]heptane (^{13}C content 90%) and is assumed to have the tagged carbon atom at least partially scrambled.[12] Although we do not know the location of the ^{13}C label in the allyl ion, the results clearly show that the three incoming carbon atoms have equal probabilities of being found in the $C_7H_7^+$ product of reaction with benzene, or in $C_8H_9^+$ from the reaction with toluene. Consequently, products formed via intermediate structure I or II are undistinguishable by this technique.

A final result from deuterium labeling is that protonation yields a single product ion in all cases; e.g.,

$$C_3H_5^+ + C_6D_6 \rightarrow C_3H_4 + C_6D_6H^+ \qquad \text{(R-5a)}$$

$$\nrightarrow C_3H_3D + C_6D_5H_2^+ \qquad \text{(R-5b)}$$

This contrasts dramatically with the tropylium (and homologues) results and provides evidence that proton transfer (reaction R-1) does not occur via the same $C_9H_{11}^+$ intermediate complex as $C_7H_7^+$ formation (reaction R-2).

C. Formation and Decomposition of $C_9H_{11}^+$ Intermediates. As discussed in the last section, the experiments using labeled reactants suggest that the $C_7H_7^+$ ion (and its homologues) are formed by mechanisms involving at least two forms of an intermediate complex $C_9H_{11}^+$. Since the latter ion was never observed as a direct product of the reactions of $C_3H_5^+$ with benzene, an upper limit for its lifetime is established as approximately 10^{-3} s. However, the observation of the adduct in high-pressure experiments suggested that it could be formed in the tandem ICR ion source. Therefore a 100/1 mixture of C_2H_4/C_6H_6 was introduced in the ion source of the tandem mass spectrometer at a pressure of ca. 10^{-2} Torr. Multiple collisions with the bath gas following formation of the adduct did, indeed, generate $C_9H_{11}^+$, implying a lifetime longer than 10^{-6} s for the intermediate complex. Injection of mass selected $C_9H_{11}^+$ into the second stage of the tandem and subsequent

decomposition of the ion in the ICR cell yields only the $C_7H_7^+$ ion. No protonated benzene was detected, thus confirming the hypothesis that formation of the latter product is independent of the $C_7H_7^+$ formation and does not proceed via a long-lived reaction complex.

The results for decomposition of $C_9H_{11}^+$ as a function of pressure in the ion source are shown in the main portion of Figure 3. The pressure dependence for the intensities of the $C_9H_{11}^+$ and $C_7H_7^+$ ions is interpreted in terms of the excess energy in the $C_9H_{11}^+$ and its effect on the unimolecular decomposition rate constant, k_4.

$$C_9H_{11}^+ \xrightarrow{k_4} C_7H_7^+ + C_2H_4 \qquad \text{(R-6)}$$

In the insert for Figure 3 we consider a hypothetical example of how such a relationship as that depicted in Figure 3 can be obtained from simple theories for unimolecular reactions.[13] If we assume that there is a small range of effective excitation energy in the $C_9H_{11}^+$ ion, the ion is characterized by a range of decomposition rates in region A of the curve of the insert. It follows that a fairly sharp decline in k_4 will result from decreasing internal excess energy in the $C_9H_{11}^+$ complex with increasing source pressure.

An average decomposition rate constant is obtained experimentally from the relationship in $I_0/I = \bar{k}_4 t$, where I_0 is the sum of $C_9H_{11}^+$ and $C_7H_7^+$ ions intensities, I is the $C_9H_{11}^+$ ion intensity, and the time t is set equal to the residence time of ions in the ICR cell (2 ms in the present experiments). Following this procedure, k_4 was plotted as a function of pressure in Figure 3. From this curve we deduce that the average decomposition rate constant for $C_9H_{11}^+$ ions prepared in this manner is a nearly exponential function of $\bar{n}$ and may be expressed as follows:

$$\bar{k}_4 = 7.5 \pm 0.04 - (0.499 \pm 0.01)\bar{n}$$

In the discussion which follows we shall attempt to relate the variation in the measured decomposition rate constant to the excess internal energy in the decomposing species $C_9H_{11}^+$. We shall ignore the small amount of decomposition of $C_9H_{11}^+$ which occurs during the 2.6 μs required for mass analysis and ion injection of the primary beam. We shall use the simplified RRK expression for the rate of a unimolecular reaction

$$k = \nu\left(\frac{E - E_0 - \bar{n}\langle\Delta E\rangle}{E}\right)^{s-1} \qquad \text{(E-1)}$$

where ν is a frequency factor, E the internal energy, E_0 the activation energy, $\langle\Delta E\rangle$ the mean energy transferred per collision, $\bar{n}$, with the bath gas, and $s - 1$ the number of effective oscillators. Assuming no activation energy barrier for R-4, a lower limit for the excess energy $E - E_0$ is given by the exothermicity of R-2, i.e., between 60 and 90 kJ/mol depending on whether $C_7H_7^+$ is formed as benzyl or tropylium. The term $s - 1$ is set equal to 18, i.e., one-third of the total number of oscillators, which is a fair approximation in large systems such as $C_9H_{11}^+$. $\langle\Delta E\rangle$ is then determined from the ratio of the decomposition rate constants according to

$$k_{4,1}/k_{4,2} = \nu\left(\frac{E - E_0 - \langle\Delta E\rangle}{E}\right)^{s-1} \Big/ \nu\left(\frac{E - E_0 - 2\langle\Delta E\rangle}{E}\right)^{s-1} \qquad \text{(E-2)}$$

where $k_{4,1}$ and $k_{4,2}$ represent the experimental values of k_4 after $C_9H_{11}^+$ has experienced one and two collisions, respectively. This treatment yields values of $\langle\Delta E\rangle$ between 1.8 and 2.4 kJ/mol for the formation of benzyl and tropylium ions, respectively. This result leads to the hypothesis that the dependence of k_4 on excess internal energy in $C_9H_{11}^+$ may be expressed approximately by the relationship

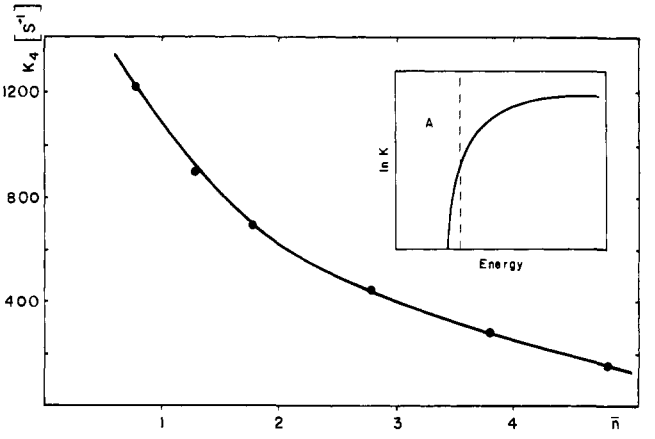

Figure 3. Decomposition rate constant k_4 as a function of $\bar{n}$. Insert: example of the dependence of decomposition rate constant k_4 upon excess internal energy (see text).

Table III. Unimolecular Decomposition Products of $C_9D_6H_5^+$ and $C_9H_6D_5^+$ Ions

	$C_9D_6H_5^+$ [a]		$C_9H_6D_5^+$ [b]	
Product	Low $\bar{n}$ [c]	High $\bar{n}$ [c]	Low $\bar{n}$ [c]	High $\bar{n}$ [c]
$C_7D_6H^+$	0.175	0.23	0.22	0.275
$C_7D_5H_2^+$	0.615	0.62	0.57	0.595
$C_7D_4H_3^+$	0.21	0.15	0.21	0.13

[a] Formed in a 1/100 mixture of C_6D_6/C_2H_4. [b] Formed in a 1/100 mixture of C_6H_6/C_2D_4. [c] Low $\bar{n}$ refers to an average of less than one collision of the ion before extraction from the source; high $\bar{n}$ refers to an average of six collisions before extraction.

$$\ln k_4 = \alpha E \qquad \text{(E-3)}$$

where E is the excess energy in kJ/mol and α has a value between 0.21 and 0.28. In view of the approximations involved further speculation concerning this empirical relationship is unwarranted at this time. However, it appears useful to us to suggest this approach for assessing the influence of excess internal energy on the lifetimes of reaction intermediates.

Some additional, preliminary experiments were conducted using 100/1 mixtures of C_2H_4/C_6D_6 and C_2D_4/C_6H_6 to form $C_9D_6H_5^+$ and $C_9H_6D_5^+$ ions, respectively. These ions were focused into the second stage of the tandem spectrometer and the decomposition product ions noted. The results are given in Table III. The tropylium ion distribution resembles the corresponding values of Table II, except for a slight increase in the intensity of the product having exchanged two protons of the original benzene molecule ($C_7D_4H_3^+$ and $C_7H_4D_3^+$, respectively). As before, a single protonated benzene ion was observed in both experiments.

Conclusions

We can now state that tropylium (and benzyl) species observed in the methane CI spectra of aromatic compounds results from $C_3H_5^+$ attack on the aromatic ring. To a much lesser extent, proton transfer from $C_3H_5^+$ can result in the formaton of a protonated species for any given aromatic. Hydride transfer channels are open only to aromatic compounds which possess alkyl side chains. The rate constants for these reactions are of the magnitude predicted by the simple ion-induced dipole model. When the internal energy of the reactant ion is reduced via nonreactive collisions, the rate of reaction is enhanced for high-pressure ethane as the source of $C_3H_5^+$ but shows no change when ethylene is used. Contrariwise, the thermodynamically stable $C_7H_7^+$ species is more favored for "relaxed" $C_3H_5^+$ from methane, ethane, propane, or isobutane, while $C_3H_5^+$ from ethylene produces more $C_7H_7^+$ at higher

internal energies. These effects are not well understood at this time.

We conclude that the metastable ion method and its results, as described above, provide an effective technique for studying the decomposition of reaction intermediates which could not be observed directly in the ICR cell. To the extent that isotope distributions probe the properties of the respective ions, the metastable ions generated at higher pressure have been shown to exhibit the same properties as reaction intermediates unobserved at low (ICR) pressures. This combination of techniques, including the labeling studies, reveals that the benzyl and tropylium ions formed most probably result from $C_9H_{11}^+$ species of structures I and II, respectively. Protonated aromatic species formed in the competing ion-molecule reaction result from simple proton transfer.

Acknowledgments. The authors are grateful to the National Science Foundation for support of this research through Grants GP 33870X and GP38125X. R.H. thanks the Fonds National Suisse for partial support. T.A.E. gratefully acknowledges support from the National Center for Toxicological Research. We are indebted to Professor T. Gäumann (EPF-Lausanne) for his generous gift of the 1-bromo[2-^{13}C]heptane.

References and Notes

(1) (a) Institut de Chimie Physique EPFL; (b) University of Utah.
(2) (a) H. M. Grubb and S. Meyerson in "Mass Spectrometry of Organic Ions", F. W. McLafferty, Ed., Academic Press, New York, N.Y., 1963, pp 516–519; (b) J. T. Bursey, M. M. Bursey, and D. G. I. Kingston, *Chem. Rev.*, **73**, 191 (1973); (c) F. W. McLafferty and J. Winkler, *J. Am. Chem. Soc.*, **96**, 5182 (1974); (d) L. P. Theard and W. H. Hamill, *ibid.*, **84**, 1134 (1962).
(3) R. P. Clow and J. H. Futrell, *J. Am. Chem. Soc.*, **94**, 3748 (1972).
(4) R. P. Clow and T. O. Tiernan, 21st Annual Conference on Mass Spectrometry and Allied Topics, San Francisco, Calif., May 20–25, 1973, Paper B-4.
(5) M. S. B. Munson and F. H. Field, *J. Am. Chem. Soc.*, **89**, 1047 (1967).
(6) D. L. Smith and J. H. Futrell, *Int. J. Mass Spectrom. Ion Phys.*, **14**, 171 (1974).
(7) (a) J. L. Franklin, J. G. Dillard, H. M. Rosenstock, J. T. Herron, K. Draxl, and F. H. Field, "Ionization Potentials, Appearance Potentials, and Heats of Formation of Gaseous Positive Ions", NSRDS-NBS 26, U.S. Government Printing Office, 1969; (b) S. E. Buttrill, Jr., A. D. Williamson, and P. LeBreton, *J. Chem. Phys.*, **62**, 1586 (1975).
(8) R. D. Smith and J. H. Futrell, *Int. J. Mass Spectrom. Ion Phys.*, **20**, 347 (1976).
(9) R. C. Dunbar, J. Shen, and G. A. Olah, *J. Am. Chem. Soc.*, **94**, 6862 (1972), and references cited therein.
(10) K. L. Rinehart, A. C. Buchholz, G. E. Van Lear, and H. L. Cantrill, *J. Am. Chem. Soc.*, **90**, 2983 (1968).
(11) R. C. Dunbar, *J. Am. Chem. Soc.*, **97**, 1382 (1975).
(12) A. Flaux, B. Wirz, and T. Gäumann, *Helv. Chim. Acta*, **57**, 708 (1974), and references cited therein.
(13) For examples of applications of the quasi-equilibrium theory of mass spectra to ion-molecule reactions, see M. L. Vestal in "Fundamental Processes in Radiation Chemistry", P. Ausloos, Ed., Interscience, New York, N.Y., 1968.

Quantitative Comparison of Theoretical Calculations with the Experimentally Determined Electron Density Distribution of Formamide

E. D. Stevens,* J. Rys, and P. Coppens

Contribution from the Department of Chemistry, State University of New York at Buffalo, Buffalo, New York 14214. *Received July 28, 1977*

Abstract: A thermally smeared theoretical electron density distribution of the formamide molecule is calculated for comparison with an experimental distribution deduced from x-ray diffraction measurements at 90 K. The theoretical density is obtained from an extended basis set wave function and smeared using the rigid body thermal motions derived from the low-temperature x-ray experiment. Agreement between theory and experiment over much of the molecule is within twice the estimated standard deviation of the experimental density. Significant differences include elongation of the experimental C–N bond peak along the bond axis, and nonbonding density peaks near the oxygen above and below the molecular plane in the experimental density. Discrepancies between theory and experiment are discussed in terms of deficiencies in the model including neglect of internal thermal motion, neglect of intermolecular interactions, lack of flexibility in the basis set, and neglect of electron correlation.

Introduction

The theoretical electron density distribution is a detailed property of a system which is sensitive to the quality of the molecular wave function. It is poorly reproduced by semiempirical or minimal basis set calculations and converges slowly to the Hartree–Fock limit as the basis set size is increased.[1,2] Since experimental electron density distributions are now available from accurate x-ray diffraction experiments, the extent to which theoretical and experimental densities agree is of interest. The agreement found for small molecules gives an indication of the reliability of experimental measurements on larger molecules for which rigorous calculations are currently impossible. Although the experimental results do not yield the wave function itself, they provide a detailed and sensitive property which any trial wave function must satisfy.

Experimental densities are smeared by thermal motion in the crystal. To compare theoretical densities with experimental measurements, we apply the thermal motion as derived from the x-ray data to the theoretical static density. This convolution removes some of the sharper features of the static density which cannot be deduced from the experimental measurements at finite resolution.

Relatively few comparisons have been made between experimental and theoretical electron density distributions.[3] Several of those published have employed limited basis sets such as the 4-31G set for tetracyanoethylene[4] and the double ζ set for thiourea,[5] which may, however, be improved by the addition of atom and bond polarization functions.[4] We have recently compared the density of the azide ion as found in NaN_3 and KN_3 with a thermally smeared large basis set theoretical density on N_3^-,[6] and report here a comparison of the experimental low-temperature density distribution of form-

0002-7863/78/1500-2324$01.00/0